


Bufalin stimulates antitumor immune response by driving tumor-infiltrating macrophage toward M1 phenotype in hepatocellular carcinoma

Zhuo Yu,¹ Yuyao Li,² Yue Li,² Jinghao Zhang,¹ Man Li,³ Longshan Ji,³ Yifei Tang,¹ Yanxi Zheng,¹ Jianguo Sheng,⁴ Qiucheng Han,⁴ Fu Li,⁵ Jianfeng Guo,⁶ Lingtai Wang,¹ Xuehua Sun,^{1,2} Yueqiu Gao,^{1,2} Hai Feng ²

To cite: Yu Z, Li Y, Li Y, *et al.* Bufalin stimulates antitumor immune response by driving tumor-infiltrating macrophage toward M1 phenotype in hepatocellular carcinoma. *Journal for ImmunoTherapy of Cancer* 2022;**10**:e004297. doi:10.1136/jitc-2021-004297

► Additional supplemental material is published online only. To view, please visit the journal online (<http://dx.doi.org/10.1136/jitc-2021-004297>).

Accepted 29 April 2022



© Author(s) (or their employer(s)) 2022. Re-use permitted under CC BY-NC. No commercial re-use. See rights and permissions. Published by BMJ.

For numbered affiliations see end of article.

Correspondence to

Prof. Hai Feng;
fogsea@163.com

Prof. Yueqiu Gao;
gaoyueqiu@shutcm.edu.cn

Prof. Xuehua Sun;
susun_sxh@shutcm.edu.cn

ABSTRACT

Background Immunotherapy for hepatocellular carcinoma (HCC) exhibits limited clinical efficacy due to immunosuppressive tumor microenvironment (TME). Tumor-infiltrating macrophages (TIMs) account for the major component in the TME, and the dominance of M2 phenotype over M1 phenotype in the TIMs plays the pivotal role in sustaining the immunosuppressive character. We thus investigate the effect of bufalin on promoting TIMs polarization toward M1 phenotype to improve HCC immunotherapy.

Methods The impact of bufalin on evoking antitumor immune response was evaluated in the immunocompetent mouse HCC model. The expression profiling of macrophage-associated genes, surface markers and cytokines on bufalin treatment *in vitro* and *in vivo* were detected using flow cytometry, immunofluorescence, western blot analysis, ELISA and RT-qPCR. Cell signaling involved in M1 macrophage polarization was identified via the analysis of gene sequencing, and bufalin-governed target was explored by immunoprecipitation, western blot analysis and gain-and-loss of antitumor immune response. The combination of bufalin and antiprogrammed cell death protein 1 (anti-PD-1) antibody was also assessed in orthotopic HCC mouse model.

Results In this study, we showed that bufalin can function as an antitumor immune modulator that governs the polarization of TIMs from tumor-promoting M2 toward tumor-inhibitory M1, which induces HCC suppression through the activation of effector T cell immune response. Mechanistically, bufalin inhibits overexpression of p50 nuclear factor kappa B (NF-κB) factor, leading to the predominance of p65-p50 heterodimers over p50 homodimers in the nuclei. The accumulation of p65-p50 heterodimers activates NF-κB signaling, which is responsible for the production of immunostimulatory cytokines, thus resulting in the activation of antitumor T cell immune response. Moreover, bufalin enhances the antitumor activity of anti-PD-1 antibody, and the combination exerts synergistic effect on HCC suppression.

Conclusions These data expound a novel antitumor mechanism of bufalin, and facilitate exploitation of a new potential macrophage-based HCC immunotherapeutic modality.

WHAT IS ALREADY KNOWN ON THIS TOPIC?

- ⇒ Tumor microenvironment (TME) plays a critical role in the development of hepatocellular carcinoma (HCC) and greatly influences the outcome of immunotherapy.
- ⇒ Bufalin exerts anti-HCC effect via the inhibition of cancer cell proliferation, while the impact on the TME remains elusive.

WHAT THIS STUDY ADDS?

- ⇒ Bufalin promotes the transition of macrophage in TME from M2 to M1 phenotype by activating nuclear factor kappa B signaling, which leads to the stimulation of immune response and synergizes with antiprogrammed cell death protein 1 antibody to suppress HCC.

HOW THIS STUDY MIGHT AFFECT RESEARCH, PRACTICE AND/OR POLICY?

- ⇒ This study explored the anti-HCC mechanism of bufalin from immune-regulation aspect and provides a promising macrophage-based immunotherapeutic strategy that enriches the knowledge of HCC treatment.

BACKGROUND

Hepatocellular carcinoma (HCC) is the second leading cause of cancer-related death worldwide.¹ Local or systemic therapy such as surgery and chemotherapy alone or in combination only show clinical efficacy in a minority of patients.^{2 3} Although immune checkpoint blockade achieved encouraging results in patients with HCC, the remission rate is <20%.⁴ Increasing studies have evidenced that immunosuppressive tumor microenvironment (TME) is responsible for such insufficient response to immunotherapy.^{5 6} The composition of immune cells infiltrated in the TME plays the critical role in manipulating the immunosuppressive characters, which induce tumor proliferation

and recurrence, and affect efficacy of immunotherapy.^{7,8} Therefore, the targeting of potential immune cells for remodeling of the TME may be a promising strategy for the improvement of immunotherapy.

Macrophages are the major immune component abundantly accumulated in the TME, and significantly impact the immunosuppressive characters of tumor lesions.⁹ They demonstrate functional plasticity and can be polarized to two distinctive phenotypes for the governing of HCC development.¹⁰ One is classically activated M1 phenotype that exhibits the tumor-inhibitory activity by producing pro-inflammatory cytokines such as interferon (IFN)- γ and tumor necrosis factor (TNF)- α .¹¹ The other is alternatively activated M2 phenotype that nurtures tumor growth via the expression of anti-inflammatory cytokines such as interleukin (IL)-10 and transforming growth factor (TGF)- β .¹² Tumor-infiltrating macrophages (TIMs) are mainly represented as immunosuppressive M2 that plays the central role in immune evasion of cancer cells. The accumulated M2-TIMs upregulate the expression of PD-L1 and generate anti-inflammatory cytokines such as IL-10, transforming growth factor (TGF)- β and Prostaglandin E2 (PGE2), leading to the exhaustion of T cell antitumor immunity.¹³ Depleting M2-TIMs or transforming M2-TIMs to M1 phenotype can effectively reduce the production of protumorigenic cytokines and signaling proteins, which ameliorates immunosuppression and reinvigorates antitumor immune response.¹⁴ Therefore, M2-TIMs serve as a good target used to exploit the feasible immunotherapy for refractory HCC cases.

Bufoalin, a derivative of steroid, is the major active component of traditional Chinese medicine *Chansu*, which is extracted from the skin and parotid venom glands of toad. Studies have shown that bufoalin exhibits antitumor activity on many cancers including HCC.^{15–17} In mouse model of hepatitis B virus-associated HCC, bufoalin downregulated the expression of androgen receptor and cell cycle-related kinase in the β -catenin/TCF signaling, leading to the direct killing of cancer cells.¹⁸ Moreover, bufoalin was also found to induce the apoptosis of human HCC cell via the targeting of JNK activation and Fas-mediated pathway.^{19,20} Recent studies have indicated an association of bufoalin-suppressed HCC proliferation and metastasis with the modulation of immune cells.²¹ However, the mechanism that bufoalin acts on immune cells within the TME and the type of cells that are involved in this process remain to be elucidated.

In present study, we evaluated the function of bufoalin on the activation of antitumor immune response in the immunocompetent orthotopic HCC mouse model compared with nude mice. Subsequently, we identified TIM as the target of bufoalin in the immune elimination of tumor cells. Further research showed that bufoalin promoted the TIM conversion from M2 to M1 by activating nuclear factor kappa B (NF- κ B) signaling, which stimulated antitumor T cell immune response through the expression of pro-inflammatory cytokines. Furthermore, we also verified that bufoalin enhanced the

antitumor activity of antiprogrammed cell death protein 1 (anti-PD-1) antibody, and the combination synergized to suppress HCC proliferation. Therefore, our findings reveal an important role of bufoalin as an immune modulator in promoting M1 polarization, and exploit a novel macrophage-based therapeutic approach for the improvement of HCC immunotherapy.

MATERIALS AND METHODS

Cell lines and reagents

Murine HCC cell line Hepa1-6 and Hepa1-6-luciferase (Luc) were cultured in high glucose Dulbecco's Modified Eagle medium (Gibco) supplemented with 10% fetal bovine serum (Hyclone), 1% penicillin and streptomycin (Hyclone) at 37°C in 5% CO₂-containing humidified incubator. Reagents used in the study are mentioned in online supplemental table S1.

Animal experiment

Six-week-old male C57BL/6 mice and BALB/c athymic nude mice were ordered from Shanghai SLAC Laboratory Animal Co., Ltd. (Shanghai, China) and received appropriate care.

The orthotopic HCC model was established through the hemisplenic injection of Hepa1-6 cells into the liver. Briefly, the spleen was exposed, tied in the middle and cut into two parts with intact vascular pedicle at both sides; 1×10^6 Hepa1-6 or Hepa1-6-Luc cells were inoculated into the liver via vascular vessel in the half spleen, and the other half was returned to abdomen to keep the immune systems competent. One week later, mice were randomly divided into different groups and treated with vehicle or 10 μ g/kg bufoalin intraperitoneally every other day in 3 weeks. Tumor weight was measured and tumor volume was calculated with $length \times width \times width / 2$. To destroy systemic immunity, tumor-bearing C57BL/6 mice were exposed to sublethal dose of 700 cGy γ -irradiation or deprived of the spleen, respectively. For in vivo depletion of macrophages, tumor-bearing C57BL/6 mice were injected intraperitoneally with 100 μ L clodronate liposomes (CL, 10 mg/mL) every 4 days, accompanied by treatment of bufoalin or vehicle. In the salvage experiment, p50 NF- κ B-packaging lentivirus was given by tail vein injection. To monitor tumor growth on different treatments such as vehicle, anti-PD-1 antibody, bufoalin and the combination, tumor-bearing mice were injected with D-luciferin (Alameda) at the indicated time and examined by fluorescent imaging using IVIS imaging system (Perkin-Elmer).

Macrophage isolation and gene expression profiling

Tumor tissues isolated from C57BL/6 mice on treatment were cut into small pieces and digested with 1 mg/mL collagenase (Sigma-Aldrich), 2 units/mL hyaluronidase (Sigma-Aldrich) and 0.1 mg/mL DNase (Sigma-Aldrich). Single cells were sorted with anti-F4/80 microbeads (Miltenyi Biotec) to get TIMs with >95% of purity. For gene

expression profiling, RNA were extracted with RNeasy MiniElute kit (Qiagen), converted into complementary DNA (cDNA) and sequenced using next-generation sequencing (Illumina). Differential expression analysis was performed using the program edgeR at $p < 0.05$ with a twofold change. The gene expression level across different samples was normalized and quantified using the function of counts per million (cpm). Gene set enrichment analysis (GSEA) was performed with GSEA by false discovery rate (FDR) q value < 0.05 . The Kyoto Encyclopedia of Genes and Genomes (KEGG) analysis was performed using the bioinformatics database in David Bioinformatics Resources (<https://david.ncicrf.gov/>).

Flow cytometry

Single cells were isolated from fresh liver and tumor tissues by gentle MACS Dissociators (Miltenyi Biotec). Fc receptors were blocked by antimouse CD16/32 (BD Pharmingen), and cells were stained with antimouse surface marker antibodies (online supplemental table S2). Flow cytometry was performed on FACS Aria Fusion platform (BD Biosciences), and data were analyzed using FlowJo software (Tree Star). The expression of surface markers was detected to identify different immune cell subsets (online supplemental table S3). Absolute numbers were calculated by multiplying frequencies obtained from flow cytometry with the total live mononuclear cell count, and then divided by liver weight. For identification of different macrophage phenotypes, surface markers were referred to online supplemental table S4.

Generation of bone marrow-derived macrophages and macrophage polarization

Bone marrow-derived macrophages (BMDMs) were isolated from the femurs of C57BL/6 mice and cultured with 20 ng/mL recombinant M-CSF (Invitrogen) in the medium for 7 days. Conditioned medium (CM) culturing Hepa1-6 cells for 48 hours was mixed with BMDMs in the presence of bufalin or vehicle for 48 hours, or CM in the absence of bufalin was cultured with naïve BMDMs for 48 hours first, followed by the addition of bufalin for another 48 hours. Supernatants were collected at the indicated time for ELISA analysis of cytokines.

Enzyme-linked immunosorbent assay

Tissue samples and cell supernatant on different treatments were collected and indicated cytokines were examined using ELISA kit (R&D systems) according to the manufacturer's instruction.

Quantitative RT-PCR

RNA was extracted from cells or tumor tissues using TRIzol reagent (Invitrogen), and reverse-transcribed to cDNA using Reverse Transcription Master kit (Invitrogen). The cDNA was amplified to detect transcript levels using SYBR Premix Ex Taq kit (TaKaRa) and 7500 real-time PCR system (Applied Biosystems). The mRNA levels were normalized by *Gapdh*, and expressed as fold

change with respect to the control. The primer sequences are shown in online supplemental table S5.

Immunohistochemistry

Fresh liver tumor tissues isolated from C57BL/6 mice were fixed in 10% formalin, dehydrated, embedded in paraffin and sliced. The sections were then deparaffinized in xylenes and rehydrated by a gradient of alcohols, followed by antigen retrieval and blockage of endogenous peroxidase activity. Tissue sections were then incubated with primary antibodies antimouse CD206 (1:500, PA5-46994, Invitrogen) and CD86 (1:200, PA5-114995, Invitrogen) for 2 hours. Chromogen development was automatically accomplished with EnVision Detection system (Agilent Dako) and images were obtained by Nikon microscope.

Immunofluorescence

BMDMs were treated with or without bufalin, or with bufalin in the presence of JSH-23, followed by fixation with 3% paraformaldehyde and permeabilization with 0.1% Triton X-100. Non-specific binding sites were blocked with 1% bovine serum albumin. Cells were incubated with primary antibodies (online supplemental table S6), and then correspondingly incubated with fluorescein isothiocyanate-conjugated or rhodamine-conjugated secondary antibodies. Nuclei were counterstained by 4',6-diamidino-2-phenylindole (Invitrogen) and images were captured by confocal microscope (Olympus).

T cell isolation and proliferation assay

Fresh murine spleen isolated from C57BL/6 mice was torn apart and passed through a 70 μ m nylon strainer (BD Falcon) to obtain single cell suspensions. CD4⁺ and CD8⁺ T cells were isolated using MagCelect Mouse CD4⁺ and CD8⁺ T cell isolation kit (MAGM202 and 203, R&D systems), respectively. For T cell proliferation assay, CD4⁺ or CD8⁺ T cells were labeled with carboxyfluorescein succinimidyl ester (CFSE, Invitrogen) and co-cultured with bufalin-primed BMDM (1:1) or bufalin-treated TIM (1:1) in the presence or absence of 2.5 μ g/mL anti-CD3 (Invitrogen) and 5 μ g/mL anti-CD28 (Invitrogen) for 3 days. CD3, CD4, CD8 and CFSE signals on T cells were detected by flow cytometry and proliferative percentage of CD4⁺ and CD8⁺ T cells were calculated by FlowJo software (Tree Star).

Immunoblotting

Cell lysates were separated by 10% sodium dodecyl sulfate-polyacrylamide gel electrophoresis, transferred into nitrocellulose membranes and immunoblotted with specific antimouse primary antibodies (online supplemental table S7), and with horseradish peroxidase-conjugated secondary antibodies. The proteins were visualized by ECL western blot analysis reagent (Thermo Pierce). The nuclear/cytosol fractionation kit (BioVision) was used to extract and separate the cytoplasmic and nuclear proteins.

Immunoprecipitation and ubiquitination assay

Macrophages were incubated with proteasome inhibitor MG132 (Sigma-Aldrich) for 30 min before harvest, and lysed in radio immunoprecipitation assay (RIPA) buffer supplemented with 20 μ M *N*-ethylmaleimide and 1 \times protease/phosphatase inhibitor cocktail (Roche). Equal amounts of protein were precleared with Protein G Dynabeads (Invitrogen), and immunoprecipitated (IP) with an anti-p50 antibody (D-17, Santa Cruz Biotechnology). For examination of p50 ubiquitination, the IP lysates were immunoblotted with anti-Ub antibody (P4D1, Santa Cruz Biotechnology). Input was used as loading control for the expression of p50 and β -actin.

Statistics

Statistical significance was determined by unpaired two-tailed Student's *t*-test or by one-way analysis of variance (with Bonferroni correction). Survival curves were generated using the Kaplan-Meier method, and compared

using the log-rank Mantel-Cox test. Data were presented as mean \pm SEM of three independent experiments. All statistical analyses were conducted using Prism V.8.0 software (GraphPad). The *p* value <0.05 was considered statistically significant.

RESULTS

Bufalin elicits anti-HCC immune response through the recruitment of macrophages

To understand the role of bufalin in immune response against HCC, we compared its antitumor effect in orthotopic models between nude mice and immunocompetent C57BL/6 mice (figure 1A). Bufalin reduced tumor volume and growth rate more efficiently in C57BL/6 mice than in nude mice (*p*<0.05; Figure 1B,C). Notably, the destruction of systemic immunity via irradiation or splenectomy could markedly impair the suppressive effect of bufalin on

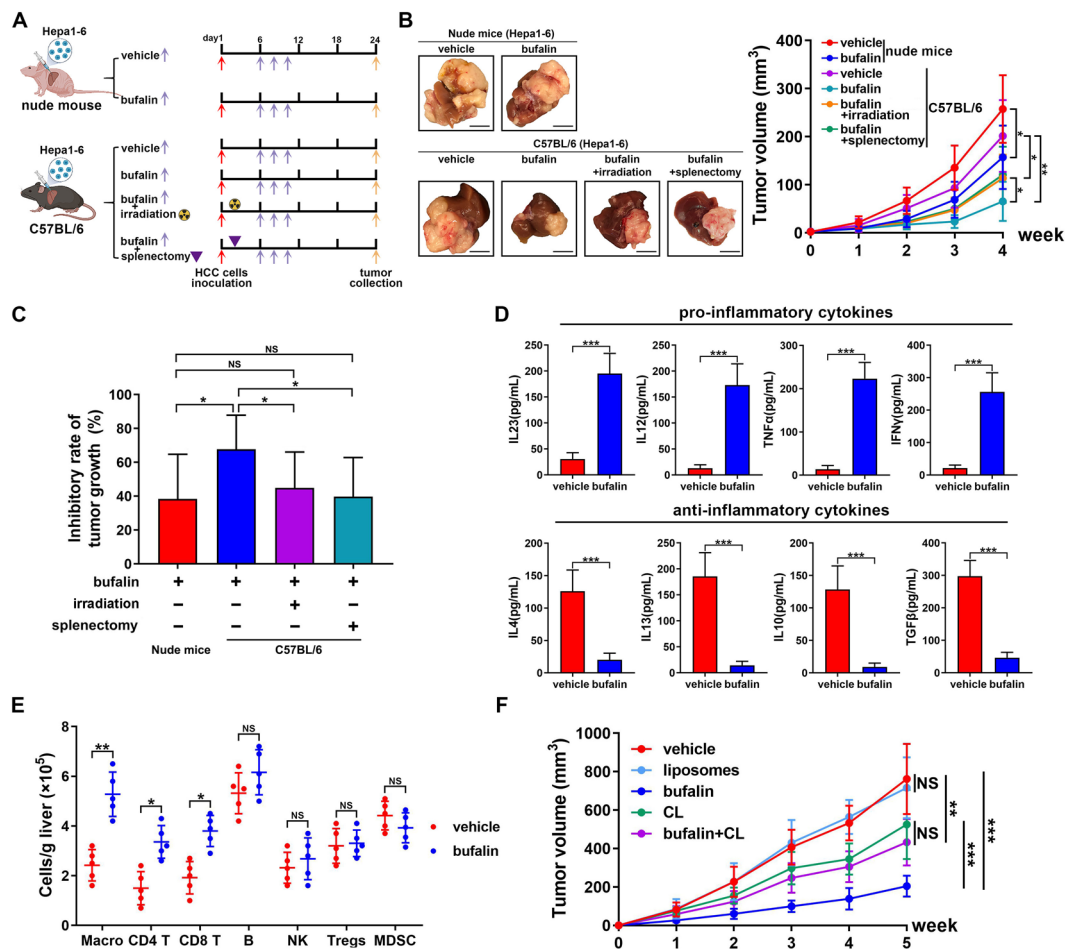


Figure 1 Bufalin induces antihepatocellular carcinoma (anti-HCC) immunity through the recruitment of macrophages. (A) Schematic diagram showed different treatments of HCC-bearing nude mice and C57BL/6 mice. (B) Nude mice and C57BL/6 mice treated by irradiation or splenectomy were given bufalin or vehicle after 1 week of the inoculation of Hepa1-6 cells in the liver (*n*=5 per group). Representative liver images are shown, and tumor growth was monitored on bufalin treatment. Scale bar=10 mm. (C) Inhibitory rates of tumor growth by bufalin in nude mice or C57BL/6 mice were calculated relative to vehicle treatment. (D) Pro-inflammatory and anti-inflammatory cytokines in the liver were measured by ELISA analysis. (E) The subsets of liver-infiltrating immune cells were measured. (F) Tumor growth was detected in HCC-bearing C57BL/6 mice treated with vehicle, liposomes, bufalin, clodronate liposomes (CL) and the combination of bufalin and CL, respectively. All data are shown as mean \pm SEM. NS, no significant; **p*<0.05, ***p*<0.01, ****p*<0.001.

HCC growth, suggesting the antitumor activity of bufalin is dependent on immune response (figure 1B,C). In addition, bufalin remarkably increased the pro-inflammatory cytokines including IL-23, IL-12, TNF- α and IFN- γ , while decreased the anti-inflammatory cytokines including IL-4, IL-13, IL-10 and TGF- β (figure 1D). Moreover, the observation that depletion of T cells with anti-CD4 or anti-CD8 neutralizing antibodies could impair the tumor-inhibitory effect of bufalin also demonstrated the involvement of immune response in its antitumor activity (online supplemental figure S1). Analysis of tumor-infiltrating immune cell subsets on bufalin treatment showed a prominent accumulation of macrophages, CD4⁺ T and CD8⁺ T cells in the liver, whereas no changes were found in other immune subsets such as B cell, natural killer, regulatory T cell and myeloid-derived suppressor cells (figure 1E). We further investigated the function of bufalin on priming recruitment of diverse immune cells. Splenic CD4⁺ or CD8⁺ T cells treated with bufalin showed no effect of proliferation (online supplemental figure S2A), suggesting that bufalin does not directly stimulate T cell immune response. In contrast, bufalin could promote macrophage proliferation, concomitant with increase of macrophage-generated IL-12 and TNF- α and decrease of IL-10 and TGF- β (online supplemental figure S2B,C). In HCC-bearing mice, macrophage deprivation by CL could effectively disrupt the inhibitory effect of bufalin on HCC growth (figure 1F), further indicating bufalin stimulates antitumor effect in a macrophage-dependent manner. These data suggest that bufalin stimulates anti-HCC immune response by priming the accumulation of macrophages.

Bufalin induces the polarization of macrophages toward M1 phenotype

We next investigated how bufalin tuned macrophages to exert antitumor effect. Flow cytometry analysis revealed bufalin recruited macrophage in tumor, and altered the composition of TIMs (figure 2A). Compared with CD206⁺ M2 predominance in TIMs on vehicle treatment, bufalin was able to convert the majority of macrophages into CD86⁺ M1 phenotype. The expression of M1-specific markers CD11c and CCR7, and costimulatory molecules CD80 and major histocompatibility complex (MHC)-II, and reduction of immunosuppressive marker PD-L1 further indicated bufalin-provoked M1 maturation and activation (figure 2B and online supplemental figure S3).²² At the transcriptional level, RNA sequencing profiling of TIMs demonstrated that bufalin treatment caused significant upregulation of aforementioned molecules and M1-associated functional markers *Ccl5*, *Cxcl9* and *Cxcl10*, but marked downregulation of M2-associated functional molecules such as *Ccl2*, *Ccl22*, *Arg1* and *Cd163* (figure 2C). Moreover, the expression of genes associated with macrophage polarization was assayed by quantitative PCR. On bufalin treatment, the levels of M1-associated genes *Nos2*, *Tnf*, *IL12b* and *Ccr7* were remarkably upregulated, while those of M2-associated genes *Arg1*, *Mgl1*, *Fizz1*

and *Ym1* were downregulated (figure 2D). Immunohistochemistry also showed the decrease of CD206 expression, but the increase of CD86 expression in TIMs on bufalin treatment, further confirming the effect of bufalin on polarizing macrophages toward M1 (figure 2E). Taken together, these findings demonstrated that bufalin is capable of polarizing macrophages to active M1.

Bufalin reprograms M2 macrophages to M1

Apart from in vivo study, we further evaluated the regulation of bufalin on macrophage polarization ex vivo. Mouse BMDMs were incubated with bufalin or vehicle in the Hepa1-6 CM for 48 hours (figure 3A). Flow cytometry analysis showed Hepa1-6 CM could mimic HCC micro-environment to polarize BMDMs toward pro-tumor M2 macrophages. However, bufalin was able to block the effect of Hepa1-6 CM and switch the BMDMs to anti-tumor M1 macrophages, concomitant with upregulation of CD80, CD11c, MHC-II and CCR7 (figure 3B and online supplemental figure S4). Immunofluorescence confirmed the effect of bufalin-polarized M1 macrophages, displaying CD86 expression and CD206 decrease (figure 3C). The IL-12/IL-10 ratio increased from 0.3 to 8 indicated the promotion of M1 polarization on bufalin treatment (figure 3D). Gene expression analysis further demonstrated that bufalin upregulated the transcription levels of M1-associated immunostimulatory cytokines *Il12* and *Tnfa*, but downregulated those of M2-associated immunosuppressive factors *Il10* and *Tgfb* (figure 3E). We then examined the influence of bufalin on polarized M2 macrophages. BMDMs were cultured in Hepa1-6 CM for 48 hours first, and then treated with bufalin for another 48 hours. M1-associated genes including *Tnfa*, *Il12*, *Cxcl10* and *Nos* were increased, while M2-associated genes including *Arg1*, *Fizz1*, *Ym1* and *Tgfb* were downregulated (figure 3F). Consistently, flow cytometry revealed upregulation of CD80, CD11c, MHC-II and CCR7, but downregulation of CD163 and ARG1 (figure 3G). Moreover, flow cytometry assay revealed the significant increase of the apoptotic number of Hepa1-6 co-cultured with bufalin-primed BMDM, while inhibition of Nitric oxide (NO) production in the BMDM could abrogate its cytotoxic effect (online supplemental figure S5). In HCC xenograft nude mice, the delivery of bufalin-primed BMDMs could effectively suppress HCC progress, while blockage of NO production abrogated the tumor-inhibitory effect (online supplemental figure S6). Collectively, these data manifested the overwhelming effect of bufalin on governing the polarization to M1 macrophages.

Bufalin stimulates T cell activation via M1 polarization

We next explored how bufalin stimulated T cell activation. CFSE-labeled splenic CD4⁺ and CD8⁺ T cells were co-cultured with bufalin-primed BMDMs in the presence or absence of anti-CD3 and anti-CD28 antibodies (figure 4A). Vehicle-primed BMDMs reduced the number of anti-CD3/anti-CD28-stimulated CD4⁺ and CD8⁺ T cells, and their production of immunostimulatory cytokines

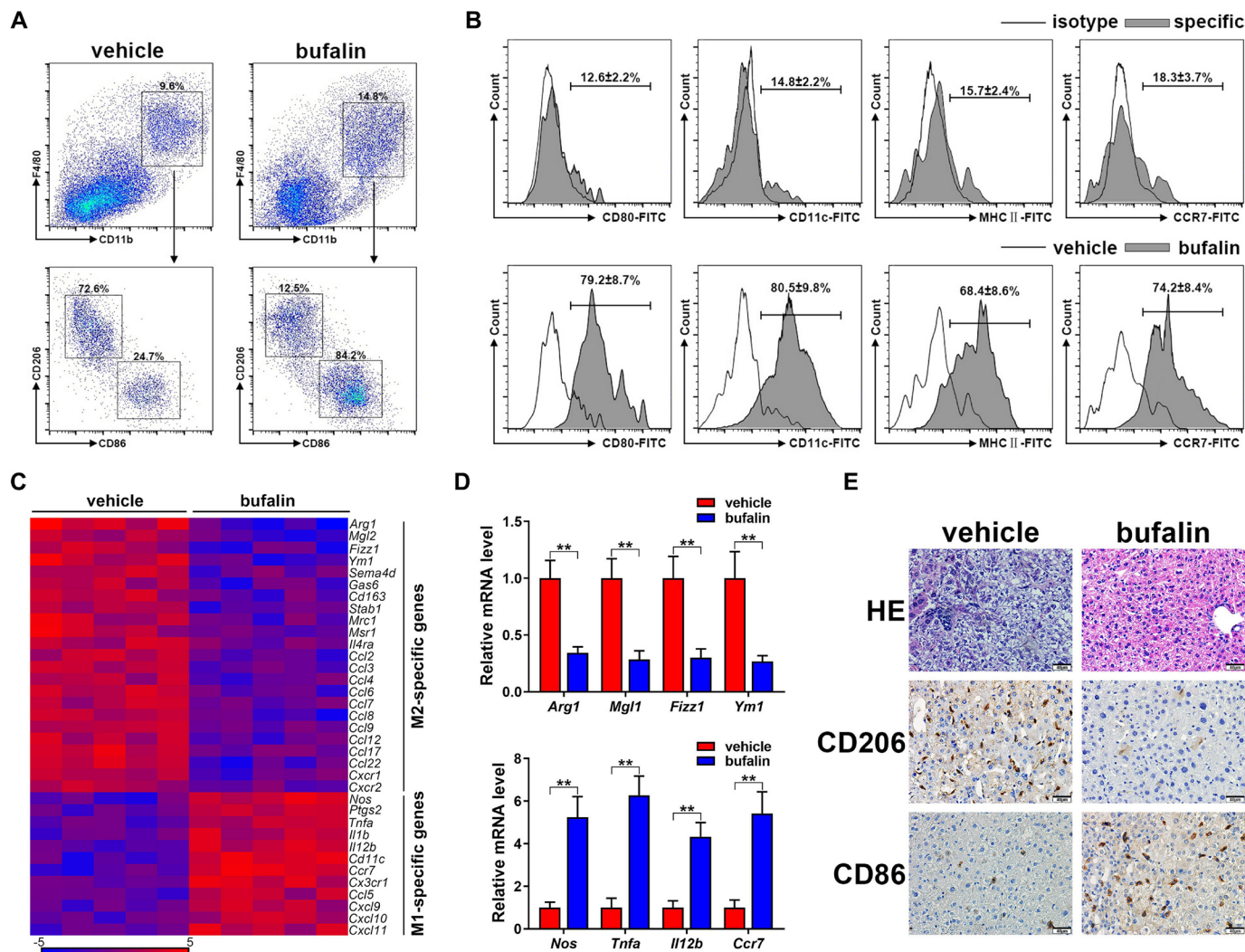


Figure 2 Bufalin drives the polarization of the recruited macrophages to M1 phenotype. (A) Tumor-infiltrating macrophages (TIMs) were isolated from the liver of hepatocellular carcinoma (HCC)-bearing C57BL/6 mice treated with vehicle or bufalin. The proportion of M1 and M2 macrophages were determined by flow cytometry (FACS). (B) The expression of M1-associated costimulatory molecules of CD80, CD11c, major histocompatibility complex (MHC)-II and CCR7 on the surface of macrophages was detected by FACS. (C) Different regulation of M1-associated and M2-associated genes from HCC tissues on vehicle or bufalin treatment was shown in hierarchical cluster heatmap. (D) Quantitative RT-PCR analysis was performed to examine the mRNA level of M1-associated and M2-associated molecules from HCC tissues on vehicle or bufalin treatment. (E) Representative histopathology and immunohistochemistry of resected HCC tissues were presented to show HCC development and tumor-infiltrating macrophages (TIMs) polarization. Scale bar=20 μ m. Data are presented as mean \pm SEM. ** P <0.01.

IFN- γ and TNF- α . Conversely, bufalin markedly induced BMDMs to promote T cell proliferation and immunostimulatory cytokines production by driving M1 polarization (figure 4B,C). Similarly, bufalin-treated TIMs isolated from tumor tissues provoked T cells proliferation and their production of immunostimulatory cytokines IFN- γ , TNF- α , IL-12 and IL-23 compared with vehicle-treated ones. Importantly, bufalin-treated TIMs provoked the proliferation of CD4⁺ and CD8⁺ T cells in the absence of anti-CD3 and anti-CD28 antibodies, suggesting these antibodies did not affect the stimulatory effect of bufalin-treated TIMs on T cell proliferation (online supplemental figures S7 and S8). In parallel, the transcription factor *T-bet* in effector CD4⁺ and CD8⁺ T cells, essential for the production of IFN- γ and TNF- α ,²³ was found to

be activated at the transcriptional and translational levels (figure 4D,E). The expression of costimulatory factor inducible T cell costimulator (ICOS) and granzyme B in CD8⁺ T cells was increased (figure 4F), suggesting bufalin-primed BMDMs promoted the proliferation of CD8⁺ T cells, and activated them into effector cells. Cell apoptosis assay further demonstrated that bufalin-primed BMDMs significantly enhanced the effect of CD8⁺ T cell on killing HCC cells compared with vehicle group either in the presence of anti-CD3 and anti-CD28 antibodies or not (online supplemental figure S9). Meanwhile, the upregulation of T helper (Th)1-associated antitumor cytokines IL-2 and IFN- γ , and the downregulation of Th2-associated pro-tumor cytokines IL-4 and IL-13 in CD4⁺ T cells co-cultured with bufalin-primed BMDMs (figure 4G), indicated that

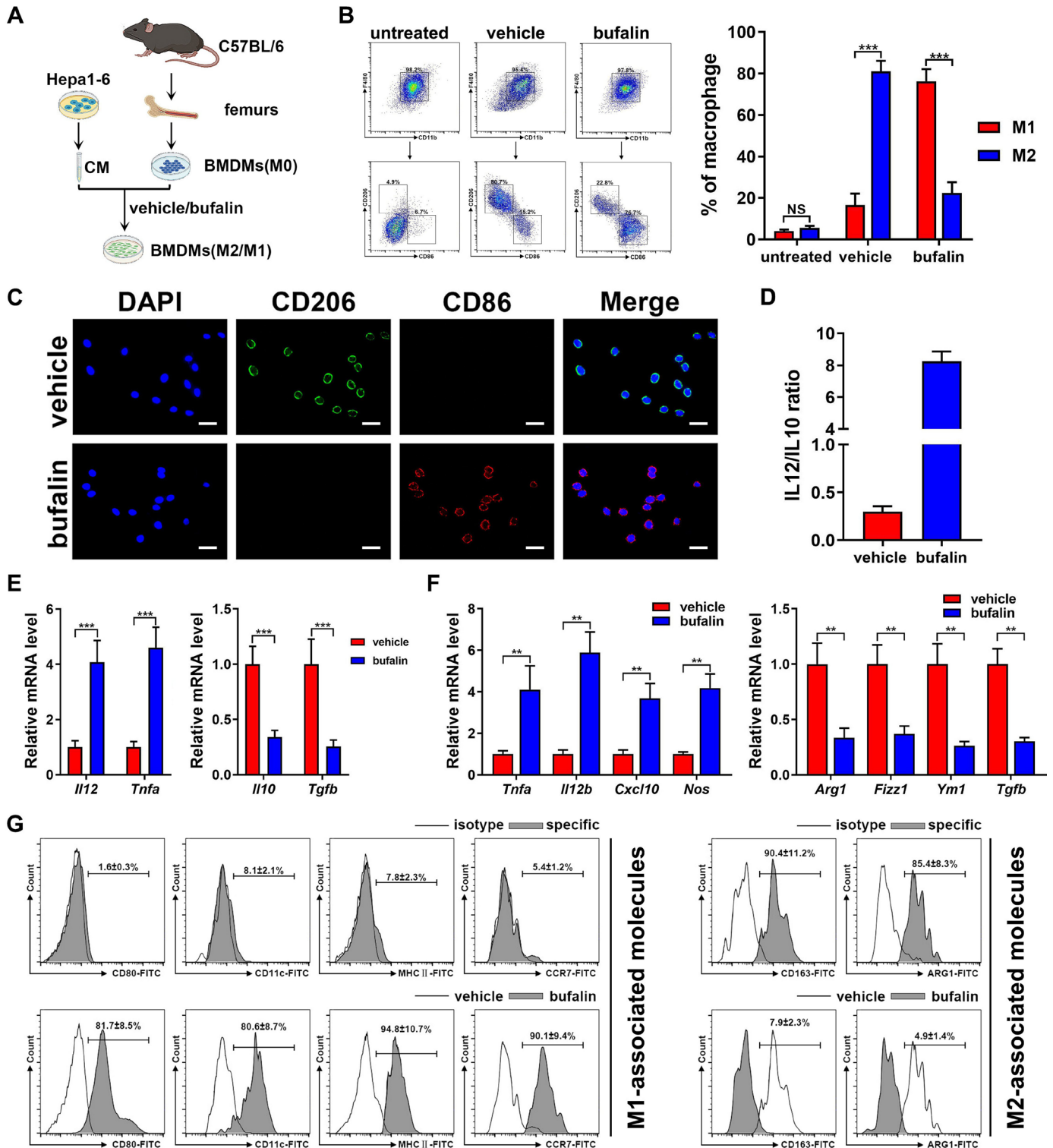


Figure 3 Bufalin drives the conversion of M2 to M1 macrophages. (A) Schematic diagram showed the polarization of macrophages affected by bufalin. (B) Bone marrow-derived macrophages (BMDMs) were treated with common medium or Hepa1-6 conditioned medium (CM) in the presence of bufalin or vehicle. The proportion of M1 and M2 macrophages were determined by flow cytometry (FACS). (C) Representative immunofluorescence images ($\times 200$ -fold) show the expression of CD206 and CD86 in the BMDMs on vehicle or bufalin treatment. 4',6-Diamidino-2-phenylindole was used to counterstain the nuclei. Scale bar=50 μ m. (D) The levels of interleukin (IL)-12 and IL-10 in the supernatant of vehicle-primed or bufalin-primed macrophages were measured by ELISA, and the IL-12/IL-10 ratio was calculated. (E) The transcription level of M1-associated and M2-associated cytokines was detected in the BMDMs on bufalin treatment. (F) The transcription level of M1-associated and M2-associated molecules was detected in Hepa1-6 CM-treated BMDMs followed by bufalin treatment. (G) FACS was performed to detect the expression of M1-associated and M2-associated molecules in Hepa1-6 CM-treated BMDMs followed by bufalin treatment. Data are shown as mean \pm SEM. * $P < 0.05$, ** $p < 0.01$, *** $p < 0.001$.

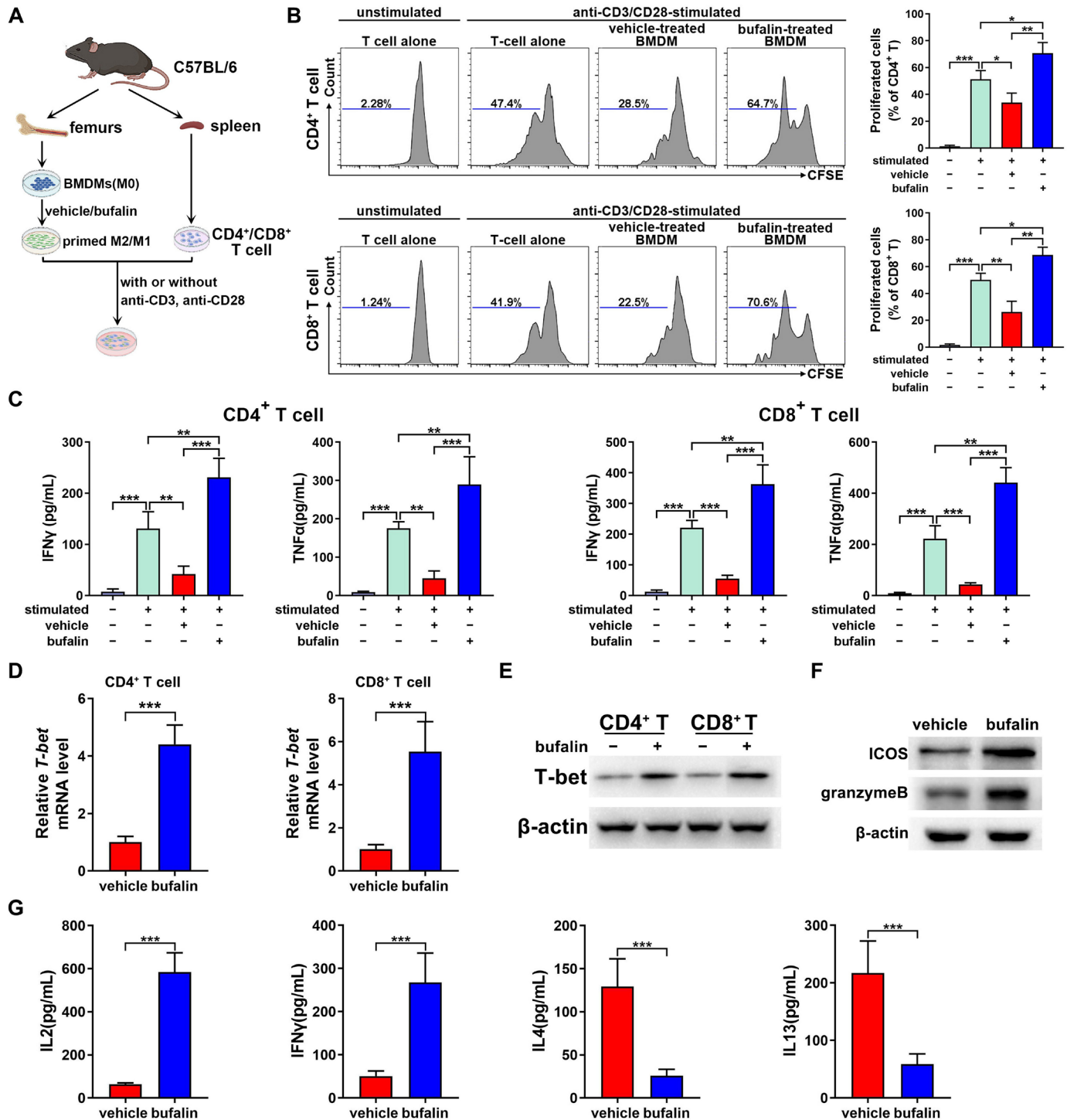


Figure 4 Bufalin provokes T cell activation and hepatocellular carcinoma (HCC) suppression via driving M1 polarization. (A) Schematic diagram showed the activity of CD4⁺ or CD8⁺ T cells affected by bufalin-primed macrophages or control. (B) The isolated CD4⁺ or CD8⁺ T cells were labeled with carboxyfluorescein succinimidyl ester (CFSE) and co-cultured with vehicle-primed or bufalin-primed bone marrow-derived macrophages (BMDMs) or alone in the presence or absence of anti-CD3 and anti-CD28 antibodies. The percentage of CFSE^{low} proliferative CD4⁺ and CD8⁺ T cells were determined by flow cytometry (FACS). (C) The secretion of interferon (IFN)- γ and tumor necrosis factor (TNF)- α from CD4⁺ or CD8⁺ T cells was examined by ELISA. (D) The mRNA level of *T-bet* in CD4⁺ and CD8⁺ T cells co-cultured with bufalin-primed BMDMs was detected by quantitative RT-PCR. (E) The protein level of T-bet in CD4⁺ and CD8⁺ T cells co-cultured with bufalin-primed BMDMs was detected by western blot analysis. (F) The protein level of ICOS and granzyme B in CD8⁺ T cells co-cultured with bufalin-primed BMDMs was detected by western blot analysis. (G) The expression of IL-2, IFN- γ , IL-4 and IL-13 released by CD4⁺ T cells co-cultured with bufalin-primed BMDMs were determined by ELISA. Data are shown as mean \pm SEM. * P <0.05, ** p <0.01, *** p <0.001.

M1 macrophages exclusively stimulated CD4⁺ Th1 cells to facilitate adaptive antitumor immunity. In HCC xenograft C57BL/6 mice, bufalin treatment promoted the migration and accumulation of T cells into tumor lesions as evidenced by immunofluorescence (online supplemental figure S10). In the gain-and-loss function experiment, replenishment of bufalin-primed BMDMs efficiently induced HCC regression in tumor-bearing mice, which was disrupted by the depletion of T cells via the delivery of anti-CD4 or anti-CD8 neutralizing antibodies (online supplemental figure S11). These results corroborated that bufalin-primed BMDM has the ability to recruit T cells into tumor lesions and provoke their anti-HCC cytotoxic effect. Together, these data demonstrated that

bufalin activates T cell immune response against HCC via M1 polarization.

Bufalin induces M1 polarization by reducing p50 NF- κ B

We next explored the molecular mechanism underlying bufalin-induced M1 macrophages. NF- κ B plays the pivotal role in the production of inflammatory cytokines associated with the regulation of macrophage function.²⁴ The functional analysis for bufalin-primed BMDMs by KEGG and GSEA showed the enrichment of bufalin-regulated genes on NF- κ B signaling pathway (figure 5A,B). NF- κ B inhibition by cardamonin could abrogate bufalin-driven switch of M2 macrophages to M1, showing the downregulation of immunostimulatory cytokines IFN- γ and TNF- α

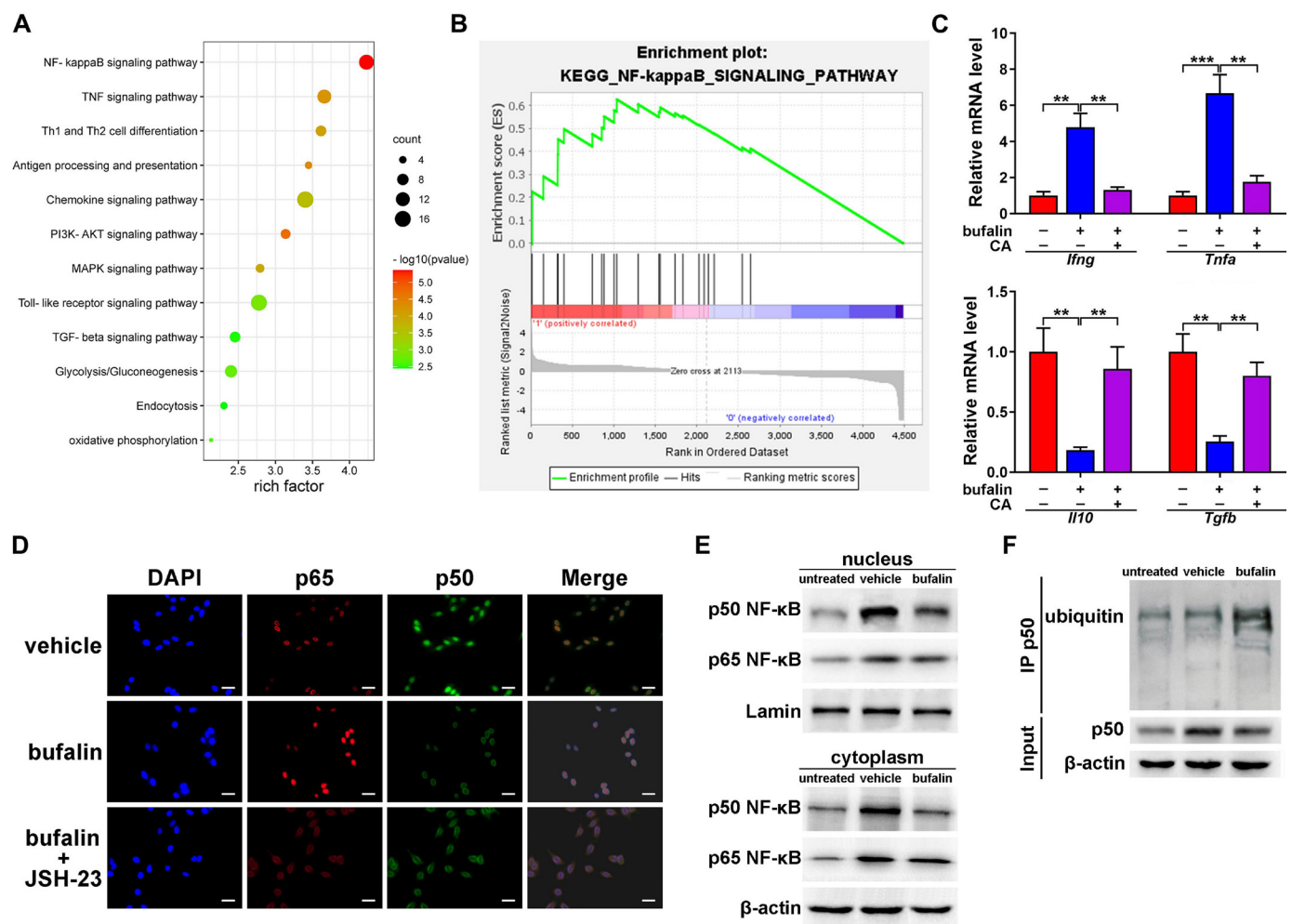


Figure 5 Bufalin inhibits p50 nuclear factor kappa B (NF- κ B) expression to drive M1 polarization. (A) Signaling pathway enrichment analysis of different expressed genes in bufalin-primed bone marrow-derived macrophages (BMDMs) was performed by KEGG. (B) Gene set enrichment analysis showed the positive significant connection of NF- κ B signaling activation with bufalin treatment compared with vehicle control. (C) The transcription level of pro-inflammatory and anti-inflammatory cytokines was detected in the vehicle-treated or bufalin-treated BMDMs in the presence or absence of cardamonin (CA). (D) Representative immunofluorescence image ($\times 200$ -fold) show the expression and distribution of p65 and p50 NF- κ B in vehicle-treated or bufalin-treated BMDMs in the presence or absence of JSH-23. Scale bar=50 μ m. (E) The expression of p50 and p65 NF- κ B in the nuclei and cytoplasm of the BMDMs on vehicle or bufalin treatment was detected by western blot analysis. Lamin and β -actin were used as loading control in the nuclei and cytoplasm, respectively. (F) Ubiquitination of p50 in vehicle-treated or bufalin-treated BMDMs were detected by western blot analysis. Equal amount of protein was immunoprecipitated by anti-p50 antibody and immunoblotted by anti-ubiquitin antibody. Data are shown as mean \pm SEM. *P<0.05, **p<0.01, ***p<0.001.

while the upregulation of immunosuppressive cytokines IL-10 and TGF- β (figure 5C). Moreover, inhibition of NF- κ B activity also impaired the effect of bufalin-primed BMDMs on promoting T cell proliferation (online supplemental figure S12). Thus, NF- κ B activation is required for the function of bufalin on M1 polarization. To elucidate the regulation of bufalin on NF- κ B activity, we assessed the impact of bufalin on the regulators controlling NF- κ B signaling. Analysis of MyD88-dependent pathway, the upstream regulators of NF- κ B signaling,²⁵ showed no detectable change in the expression of MyD88, IRAK and TRAF in bufalin-primed BMDMs (online supplemental figure S13A), suggesting bufalin could not influence this pathway. The modulation of bufalin on other negative regulators of NF- κ B signaling such as SIGIRR, ST2, SOCS1 and SHIP was also assessed,^{26 27} and no alteration was found on bufalin treatment (online supplemental figure S13B). Inhibitor of NF- κ B alpha (I κ B α) degradation is the key event in the process of NF- κ B activation; however, the level of I κ B α in bufalin-primed BMDMs was similar to that in vehicle group (online supplemental figure S13C), indicating I κ B α was not yet the target of bufalin.

The entry of p65-p50 heterodimer into the nucleus is the hallmark of NF- κ B activation to produce immunostimulatory cytokines, whereas p50 homodimer serves as a repressor to block NF- κ B activity in the nucleus.^{28 29} We thus examined the distribution of p65-p50 and p50-p50 in BMDMs, and found bufalin promoted the transfer of p65 into the nucleus but decreased p50 localization in the nucleus (figure 5D). However, bufalin-driven p65 entry could be blocked by JSH-23, a p65 NF- κ B inhibitor, implying that bufalin might indirectly tune p65 nuclear translocation. Western blot analysis of cytoplasmic and nuclear fractionation further revealed unchangeable expression of p65 on bufalin treatment, but reduction of p50 expression in line with their decrease in the nucleus (figure 5E), supporting that bufalin promoted p65 predominance in the nucleus by decreasing p50 in the BMDMs. However, gene expression analysis showed no significant alteration of *p50* mRNA levels after bufalin treatment (online supplemental figure S14), indicating bufalin could not affect p50 expression at the transcriptional level. As p50 ubiquitination and degradation is the key event associated with p50 DNA-binding affinity,³⁰ we examined whether bufalin affects p50 ubiquitination. The significant increase of p50 ubiquitination on bufalin treatment confirmed the role of bufalin in decreasing p50 homodimer via p50 degradation (figure 5F). These data demonstrate that p50 is the target of bufalin to govern macrophage polarization toward M1.

p50 overexpression abrogates bufalin-induced M1 macrophage-mediated T cell immunity

We further elucidated the role of p50 in mediating bufalin-induced M1 polarization using ectopic expression approach. Bufalin activated NF- κ B signaling, leading to the upregulation of IFN- γ and TNF- α . In contrast, constitutive overexpression of p50 in the BMDMs counteracted the effect of bufalin,

thus decreasing the expression of M1-associated genes such as *Ifng*, *Tnfa*, *Il12b*, *Cxcl10*, *Nos* (figure 6A). Consistently, the number of CD163⁺CD206⁺ M2 macrophages increased sharply as evidenced by flow cytometry, reversing the predominance of bufalin-primed M1 macrophages (figure 6B). The data confirmed that bufalin indeed promotes M1 polarization via p50 suppression. We then validated the results in vivo. In HCC-bearing mouse models, p50 overexpression remarkably impaired the tumor-inhibitory effect of bufalin, showing the promotion of tumor formation and the reduction of overall survival (figure 6C,D). In parallel, the proportion of tumor-promoting M2 macrophages greatly dominated the TIMs in bufalin-treated tumors after p50 overexpression (figure 6E). The accumulation of bufalin-induced CD4⁺ and CD8⁺ T cells in the TME was also abrogated by p50 overexpression, concomitant with downregulation of CD4⁺ Th1-associated chemokine receptor CXCR3 and chemokine CCR5, and of CD8⁺ T cell-associated chemokine receptor CXCR6 and chemokine CCL5 (figure 6F,G). In addition to the chemokines, we also found the marked reduction of antitumor cytokines IFN- γ and IL-2 in CD4⁺ T cells, and of stimulatory molecules ICOS and granzyme B in CD8⁺ T cells as well (figure 6H), indicating the exhaustion of T cell antitumor activity. Together, these data suggest that bufalin drives M1 polarization for the activation of anti-HCC T cell immunity by inhibiting p50 expression.

Bufalin enhances the anti-HCC effect in combination with anti-PD-1 antibody

In order to overcome drug resistance and maximize therapeutic effect, combination of immunomodulatory drugs dealing with diverse immune cells is a common approach in the treatment of such refractory solid cancer as HCC. Therefore, we assessed the effect of bufalin combined with low-dose immune checkpoint inhibitor anti-PD-1 antibody (anti-PD-1 Ab) in HCC-bearing mouse models. Hepa1-6-Luc cells were inoculated into the livers of C57BL/6 mice, followed by the treatment of vehicle, bufalin, anti-PD-1 Ab and combination, respectively. Luminescent intensity analysis showed that compared with bufalin treatment, anti-PD-1 Ab alone exhibits less efficacy on suppressing tumor growth (figure 7A,B), partially due to the lower expression of PD-1 on the surface of T cells in immunosuppressive HCC microenvironment.³¹ In contrast, combination therapy of bufalin and anti-PD-1 Ab generated best effect on tumor suppression, and significantly prolonged overall survival of tumor-bearing mice compared with individual treatment, as evidenced by the survival rate of four out of five in combination, two out of five in bufalin treatment, none in anti-PD-1 Ab and vehicle, in the end of 30 days observation (figure 7C). In agreement with augmentation of HCC suppression, combination therapy markedly upregulated immunostimulatory cytokines IFN- γ and TNF- α while downregulated immunosuppressive cytokines IL-10 and TGF- β at both transcriptional and translation levels (figure 7D,E), confirming their higher ability to mobilize macrophage and T cells for the synergistic stimulation of

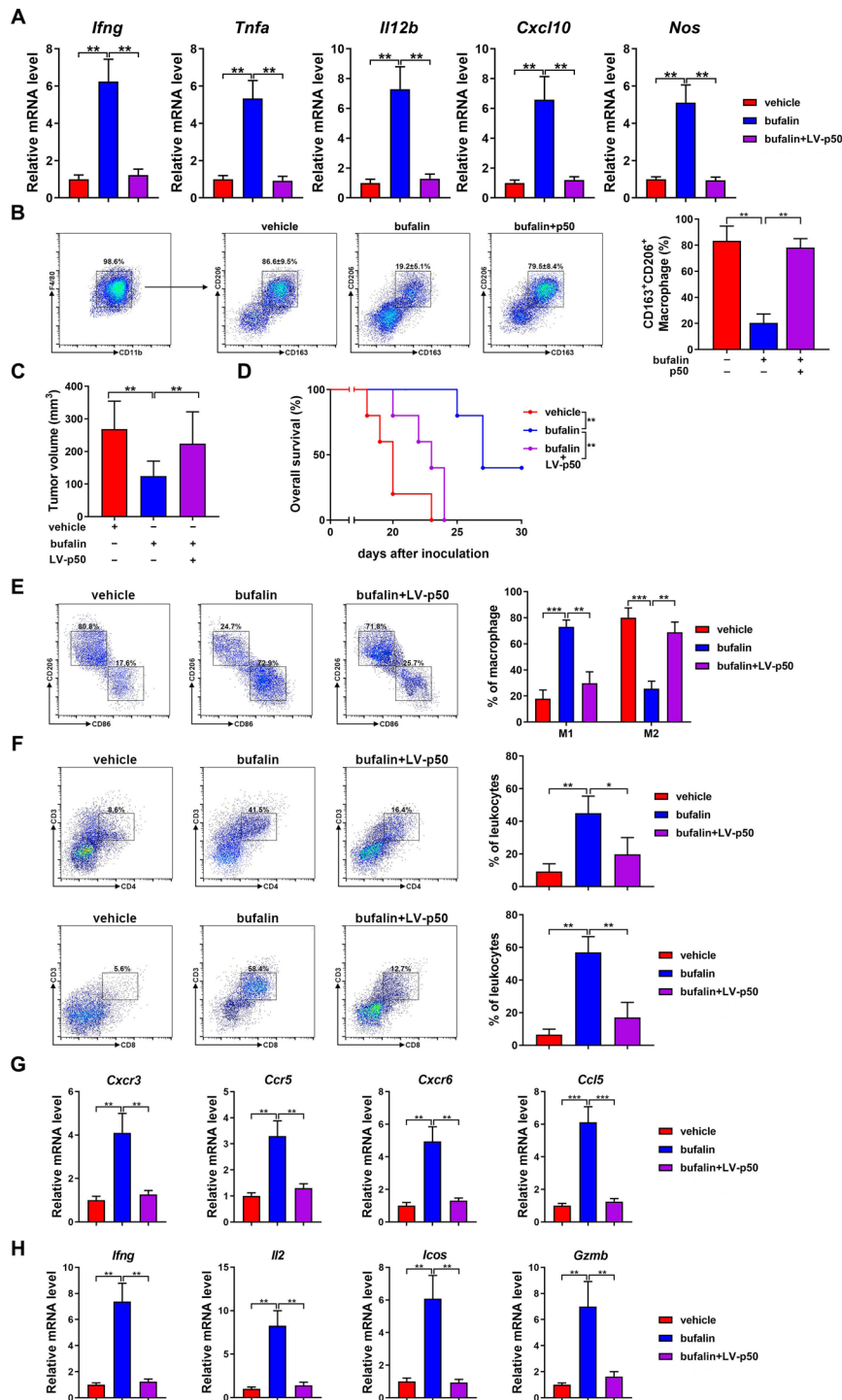


Figure 6 Overexpression of p50 nuclear factor kappa B (NF- κ B) blocks the macrophage-dependent T cell activation induced by bufalin. (A) The transcription level of M1-associated pro-inflammatory cytokines and stimulatory factors was detected in the vehicle-treated or bufalin-treated bone marrow-derived macrophages (BMDMs) transfected with p50-expressing plasmid or vector control. (B) Flow cytometry (FACS) was performed to detect the effect of p50 overexpression on reversing bufalin-driven M1 polarization to M2 macrophage. (C) Tumor volumes were detected in the hepatocellular carcinoma (HCC)-bearing C57BL/6 mice on vehicle or bufalin treatment with or without p50 NF- κ B delivery for 5 weeks ($n=5$). (D) Overall survival of the above mice with different indicated treatment was assessed. (E) The effect of p50 overexpression on the proportion of M1 and M2 macrophages in the liver tumor was determined by FACS in HCC-bearing mice with different treatments. (F) The effect of p50 overexpression on the percentage of CD4⁺ and CD8⁺ T cells in the liver tumor was examined by FACS in HCC-bearing mice with different treatments. (G) The transcription level of the chemokines *Cxcr3*, *Ccr5*, *Cxcr6* and *Ccl5*, or (H) of antitumor cytokines *Ifng* and *Il2*, and stimulatory molecules *Icos* and *Gzmb* was detected by quantitative RT-PCR in the liver tumor on vehicle or bufalin treatment with or without p50 overexpression. Data were presented as mean \pm SEM. * $P<0.05$, ** $p<0.01$, *** $p<0.001$.

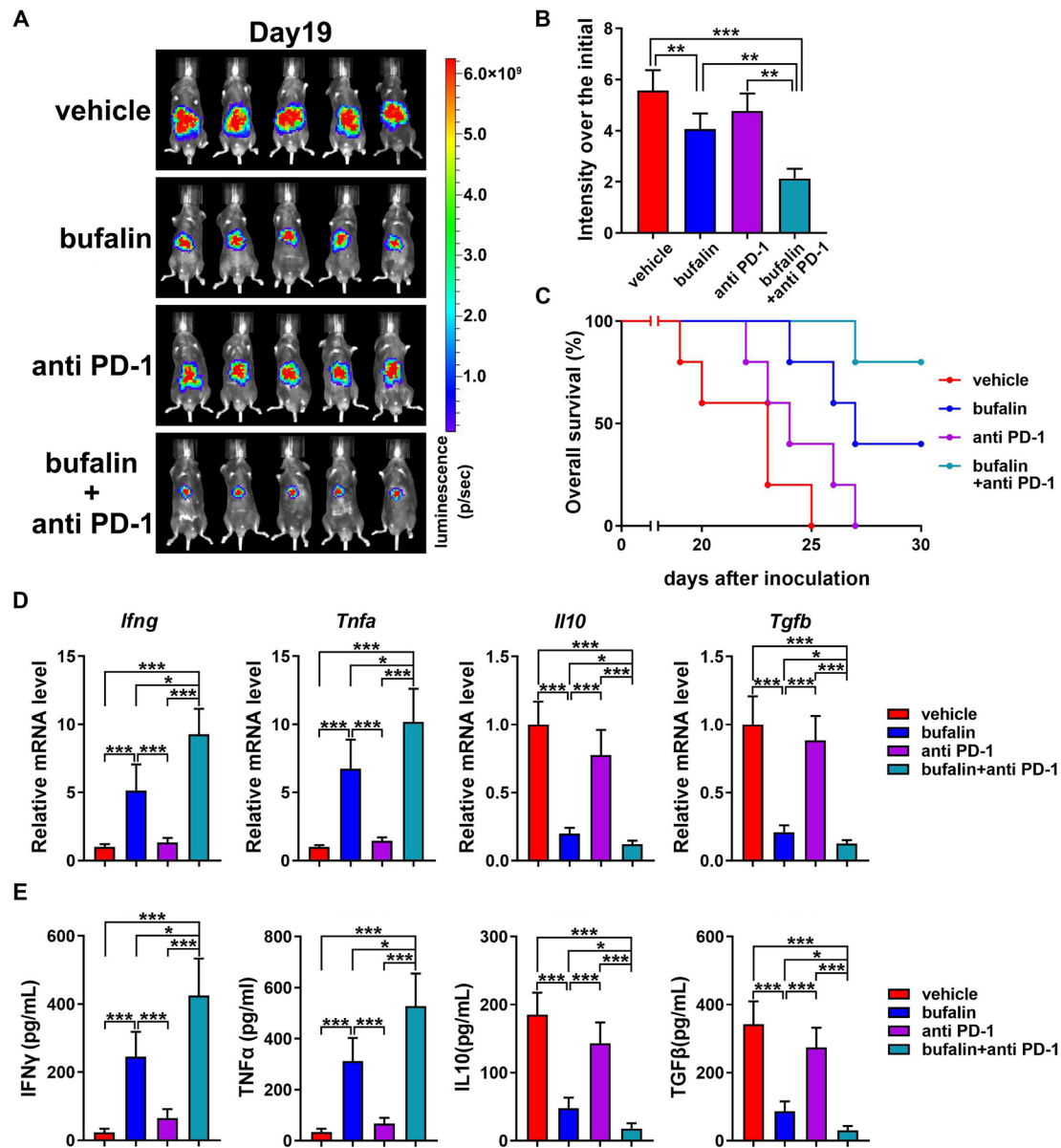


Figure 7 Bufalin enhances the antitumor efficacy in the combination with antiprogrammed cell death protein 1 (anti-PD-1) antibody (Ab). (A) Hepatocellular carcinoma (HCC)-bearing C57BL/6 mice were treated with vehicle, bufalin, anti-PD-1 Ab and the combination. Bioluminescence images of livers in various groups are shown at day 19 after HCC cell inoculation (n=5). (B) Tumor volume in various groups was measured at the end of the experiments. (C) Overall survival of HCC-bearing mice in various groups was assessed. (D) The transcription level and (E) the expression of inflammatory cytokines interferon (IFN)- γ , tumor necrosis factor (TNF)- α , interleukin (IL)-10 and transforming growth factor (TGF)- β in the liver tumor with different treatment were measured by quantitative RT-PCR and ELISA, respectively. Data are presented as mean \pm SEM. *P<0.05; **p<0.01; ***p<0.001.

antitumor immunity. Taken together, these data suggest that combining anti-PD-1 Ab and bufalin can further potentiate their beneficial effect on anti-HCC activity.

DISCUSSION

Bufalin, the major active component of *Chansu*, has been used in the treatment of various cancers in China and evaluated in clinical trials for potential anti-HCC therapy.³² Its antitumor mechanism has been ascribed to its stimulatory effect on the apoptosis and autophagy of HCC cells.³³ However, these studies selectively focused on the function

of bufalin on directly suppressing cancer cells, ignoring its immunomodulatory role in mobilizing immune cells for the antitumor effect. In the present study, we demonstrate that immune elements actually dominate the antitumor efficacy of bufalin, and provide clear evidence that bufalin conducts antitumor effect through the immune-regulating function.

Consistent to previous studies, we confirmed the anti-HCC efficacy of bufalin in HCC-bearing mouse models. However, such antitumor effect was spoiled in macrophage-deficient condition, suggesting that

bufalin activates antitumor immunity in a macrophage-mediated manner. Generally, macrophages exhibit immunomodulatory plasticity as represented by M1 and M2 phenotypes, which mediate pro-inflammatory and anti-inflammatory functions, respectively.³⁴ In HCC, the immunosuppressive microenvironment specificity can efficiently favor the polarization of macrophages toward M2, which dominate in the population of immune cells to exacerbate tumor progress.¹⁰ Therefore, M2 macrophages in the TME are an ideal target in HCC therapy and current studies mostly concentrate on the strategies of depleting M2 macrophages, for instance, by blocking CCL2/CCR2 pathway.³⁵ In our study, we also found the inhibitory effect of bufalin on M2 macrophage recruitment and activation; however, the number of TIMs failed to decrease on bufalin treatment. On the contrary, the population of macrophages increased in the tumor on bufalin treatment, suggesting the regulation of bufalin on macrophages is not merely restricted in the depletion of M2 macrophages. Further analyses showed that the increased macrophages predominantly express M1-associated markers and immunostimulatory cytokines, which confirmed the immunomodulatory effect of bufalin on governing macrophage differentiation to M1. Beyond inducing the de novo polarization to M1 subpopulation from BMDMs, bufalin reprogrammed local M2 to M1 in the TME rather than depleting them. The latter regulation showed great advantage on the HCC immunotherapy because bufalin converted tumor accomplices into tumor killers, relatively increasing the number of stimulatory immune cells. After bufalin treatment, M2 macrophages were mostly reprogrammed to M1. Subsequently, CD8⁺ T and CD4⁺ Th1 were significantly recruited and activated to reconstruct antitumor immune microenvironment. This undoubtedly relieved the immunosuppressive state and reinvigorated the antitumor immunity against HCC. Thus, our findings provide new evidence of the anti-HCC mechanism of bufalin and identify bufalin as a tumor immunotherapeutic agent.

NF- κ B is a master regulator of inflammation and immunity, and its activation in the TIM is linked with tumorigenesis. Previous studies suggested a tumor-promoting role for NF- κ B activation in TIMs, and inhibition of NF- κ B activity through IKK β deletion or I κ Ba overexpression resulted in a marked reduction of tumor formation.^{36,37} Additionally, TIM-elicited NF- κ B signal has been reported to provoke PD-L1 expression in cancer cells, while the treatment combining anti-PD-L1 antibody with NF- κ B inhibition efficiently induced cancer regression.³⁸ However, these results seemed to conflict with the production of pro-inflammatory cytokines and antitumor activity in M1 macrophage on NF- κ B activation.¹⁴ Further analysis of composition in TIM discovered the M2 predominance in these experimental carcinogenesis models.³⁹ Blockade of NF- κ B activation could switch TIMs from M2 to M1, which was associated with the reduction of NF- κ B subunit p50.²⁴ Furthermore, TIM from p50-deficient mice regained a M1 phenotype associated with tumor

reduction, accompanied by the restoration of canonical NF- κ B activity.⁴⁰ In our study, we found NF- κ B activation in the bufalin-treated macrophages, concomitant with the expression of M1-associated pro-inflammatory cytokines and molecules markers, corroborating the linkage between bufalin-induced M1 polarization and its stimulatory effect on NF- κ B signaling activity. In-depth study revealed that p50 was the target of bufalin, the overexpression of which was suppressed by bufalin-induced ubiquitination, leading to compensatory formation and translocation of p65-p50 into the nuclei of macrophages. The increase of p65-p50 in the nuclei promoted the release of immunostimulatory cytokines, and subsequently induced the activation of antitumor T cell immune response. In contrast, recovery of p50 overexpression was sufficient to thwart the inflammation and immunity induced by bufalin via the macrophage-dependent way in the TME. Thus, we confirmed that bufalin reprograms macrophages from tumor-promoting M2 to tumor-inhibitory M1 via suppressing p50 overexpression, which promotes effector T cell infiltration into the tumor and ameliorates the immunosuppressive tumor microenvironment, leading to efficient killing of tumor cells.

PD-1 is the critical immune checkpoint molecule that negatively regulates T cell immune response, and immune checkpoint inhibitors against PD-1 represent a promising therapeutic option for patients with cancers.⁴¹ However, the therapeutic efficacy of anti-PD-1 Ab achieves less beneficial response to HCC treatment due to low activation of effector T cells in the immunosuppressive TME.⁴² Drug combination is a useful strategy to improve therapeutic efficacy of monotherapy by mutually empowering multiple key targets in a tumorigenic pattern. In present study, we performed the combination treatment with bufalin and anti-PD-1 Ab on the HCC-bearing mice, and evaluated the contribution of bufalin to anti-PD-1 Ab-suppressed tumor formation. In comparison with less efficiency in the monotherapy of anti-PD-1 Ab, the addition of bufalin effectively enhances the antitumor activity of anti-PD-1 Ab, evidenced by significant suppression of tumor growth in vivo. Concurrently, the overall survival time of mice significantly prolongs after combination treatment, further corroborating that bufalin facilitates to overcome the resistance of anti-PD-1 Ab in the treatment of HCC. These effects may be ascribed to the ability of bufalin to drive the conversion of M2 to M1 macrophages, leading to improvement of immunosuppressive microenvironment and enhancement of immune activity of effector T cells in the tumor. As evidence, we confirmed that bufalin promotes the production of pro-inflammatory cytokines in the tumor, and stimulates the recruitment and activation of cytotoxic CD8⁺ T and CD4⁺ Th1 cells in macrophage-dependent manner. Activated immune T cells increase the expression of PD-1 on the surface, which increase the sensitivity to anti-PD-1 Ab treatment.

CONCLUSIONS

In summary, our data demonstrated that bufalin, by virtue of its ability to suppress the overexpression of p50 NF- κ B, to recruit macrophages into the tumor site and to govern their polarization from M2 to M1 phenotype, leads to the activation of antitumor T cell immune response in a macrophage-dependent manner. These findings unveil that bufalin actually functions as an immune modulator exhibiting the antitumor effect and shed light on a new avenue for cancer immunotherapy.

Author affiliations

¹Department of Liver Disease, Shuguang Hospital Affiliated to Shanghai University of Traditional Chinese Medicine, Shanghai, 201203, People's Republic of China

²Institute of Infectious Disease, Shuguang Hospital Affiliated to Shanghai University of Traditional Chinese Medicine, Shanghai, 201203, People's Republic of China

³Laboratory of Cellular Immunity, Shuguang Hospital Affiliated to Shanghai University of Traditional Chinese Medicine, Shanghai, 201203, People's Republic of China

⁴Department of Ultrasound, Shuguang Hospital Affiliated to Shanghai University of Traditional Chinese Medicine, Shanghai, 201203, People's Republic of China

⁵Department of Hepatopancreatobiliary Surgery, Shuguang Hospital Affiliated to Shanghai University of Traditional Chinese Medicine, Shanghai, 201203, People's Republic of China

⁶School of Pharmaceutical Sciences, Jilin University, Changchun, 130021, People's Republic of China

Acknowledgements We would like to express our gratitude to Shawn Chang (Pennsylvania State University, USA) for critical reading and English language editing of the manuscript.

Contributors ZY conceived all experiments, performed the experiments, acquired the data and drafted the paper. YuyL, YueL, JZ, LJ and JG performed part of experiments and acquired the data. YT, YZ and FL analyzed and interpreted the data. JS and QH conducted bioinformatics analysis on gene expression profiling. ML and LW provided administrative, technical and material support. XS provided study concept and design, and supervised the experiments. YG provided study concept and design, supervised the experiments and gave the final approval of the manuscript. HF provided study concept and design, supervised the experiments and revised the manuscript for important intellectual content. HF is responsible for the overall content as the guarantor. All authors have approved the final article as submitted.

Funding This work was supported by National Natural Science Foundation of China (No. 82074154, 81774240, 81874436, 81904017, 81904117); Three-year Action Plan for the Development of Chinese Medicine in Shanghai (No. ZY (2018-2020)-CCCX-2003-01); Shanghai Key Clinical Specialty Construction Project (No. shslczdzk01201); The Siming Scholar from Shanghai Shuguang Hospital (No. SGXZ-201904); Youth Tip-top Talent program in Shanghai, and Xinglin Youth Scholar from Shanghai University of Traditional Chinese Medicine.

Competing interests None declared.

Patient consent for publication Not applicable.

Ethics approval Study design was approved by the animal experimentation ethics committee of Shanghai University of Traditional Chinese Medicine, and all animal experimental protocols were in compliance with the institution's guidelines.

Provenance and peer review Not commissioned; externally peer reviewed.

Data availability statement All data relevant to the study are included in the article or uploaded as supplementary information.

Supplemental material This content has been supplied by the author(s). It has not been vetted by BMJ Publishing Group Limited (BMJ) and may not have been peer-reviewed. Any opinions or recommendations discussed are solely those of the author(s) and are not endorsed by BMJ. BMJ disclaims all liability and responsibility arising from any reliance placed on the content. Where the content includes any translated material, BMJ does not warrant the accuracy and reliability of the translations (including but not limited to local regulations, clinical guidelines, terminology, drug names and drug dosages), and is not responsible for any error and/or omissions arising from translation and adaptation or otherwise.

Open access This is an open access article distributed in accordance with the Creative Commons Attribution Non Commercial (CC BY-NC 4.0) license, which permits others to distribute, remix, adapt, build upon this work non-commercially, and license their derivative works on different terms, provided the original work is properly cited, appropriate credit is given, any changes made indicated, and the use is non-commercial. See <http://creativecommons.org/licenses/by-nc/4.0/>.

ORCID iD

Hai Feng <http://orcid.org/0000-0001-9820-7111>

REFERENCES

- 1 Siegel RL, Miller KD, Jemal A. Cancer statistics, 2020. *CA Cancer J Clin* 2020;70:7–30.
- 2 Huang A, Yang X-R, Chung W-Y, *et al.* Targeted therapy for hepatocellular carcinoma. *Signal Transduct Target Ther* 2020;5:146.
- 3 Yoh T, Seo S, Taura K, *et al.* Surgery for recurrent hepatocellular carcinoma: achieving long-term survival. *Ann Surg* 2021;273:792–9.
- 4 Forner A, Reig M, Bruix J. Hepatocellular carcinoma. *Lancet* 2018;391:1301–14.
- 5 Kurebayashi Y, Ojima H, Tsujikawa H, *et al.* Landscape of immune microenvironment in hepatocellular carcinoma and its additional impact on histological and molecular classification. *Hepatology* 2018;68:1025–41.
- 6 Lu C, Rong D, Zhang B, *et al.* Current perspectives on the immunosuppressive tumor microenvironment in hepatocellular carcinoma: challenges and opportunities. *Mol Cancer* 2019;18:130.
- 7 Binnewies M, Roberts EW, Kersten K, *et al.* Understanding the tumor immune microenvironment (TIME) for effective therapy. *Nat Med* 2018;24:541–50.
- 8 Chan L-K, Tsui Y-M, Ho DW-H, *et al.* Cellular heterogeneity and plasticity in liver cancer. *Semin Cancer Biol* 2021;2.
- 9 Ostuni R, Kratochvill F, Murray PJ, *et al.* Macrophages and cancer: from mechanisms to therapeutic implications. *Trends Immunol* 2015;36:229–39.
- 10 Sica A, Invernizzi P, Mantovani A. Macrophage plasticity and polarization in liver homeostasis and pathology. *Hepatology* 2014;59:2034–42.
- 11 De Palma M, Lewis CE. Macrophage regulation of tumor responses to anticancer therapies. *Cancer Cell* 2013;23:277–86.
- 12 Biswas SK, Mantovani A. Macrophage plasticity and interaction with lymphocyte subsets: cancer as a paradigm. *Nat Immunol* 2010;11:889–96.
- 13 Li X, Yao W, Yuan Y, *et al.* Targeting of tumour-infiltrating macrophages via CCL2/CCR2 signalling as a therapeutic strategy against hepatocellular carcinoma. *Gut* 2017;66:157–67.
- 14 Mantovani A, Marchesi F, Malesci A, *et al.* Tumour-associated macrophages as treatment targets in oncology. *Nat Rev Clin Oncol* 2017;14:399–416.
- 15 Li H, Hu S, Pang Y, *et al.* Bufalin inhibits glycolysis-induced cell growth and proliferation through the suppression of integrin β 2/FAK signaling pathway in ovarian cancer. *Am J Cancer Res* 2018;8:1288–96.
- 16 Yu Z, Feng H, Sun X, *et al.* Bufalin suppresses hepatocarcinogenesis by targeting β -catenin/TCF signaling via cell cycle-related kinase. *Sci Rep* 2018;8:3891.
- 17 Zhang Y, Dong Y, Melkus MW, *et al.* Role of P53-senescence induction in suppression of LNCaP prostate cancer growth by cardiogenic compound bufalin. *Mol Cancer Ther* 2018;17:2341–52.
- 18 Yu Z, Feng H, Zhuo Y, *et al.* Bufalin inhibits hepatitis B virus-associated hepatocellular carcinoma development through androgen receptor dephosphorylation and cell cycle-related kinase degradation. *Cell Oncol* 2020;43:1129–45.
- 19 Qi F, Inagaki Y, Gao B, *et al.* Bufalin and cinobufagin induce apoptosis of human hepatocellular carcinoma cells via Fas- and mitochondria-mediated pathways. *Cancer Sci* 2011;102:951–8.
- 20 Hu F, Han J, Zhai B, *et al.* Blocking autophagy enhances the apoptosis effect of bufalin on human hepatocellular carcinoma cells through endoplasmic reticulum stress and JNK activation. *Apoptosis* 2014;19:210–23.
- 21 Yang Z, Tao Y, Xu X, *et al.* Bufalin inhibits cell proliferation and migration of hepatocellular carcinoma cells via APOBEC3F induced intestinal immune network for IgA production signaling pathway. *Biochem Biophys Res Commun* 2018;503:2124–31.
- 22 Murray PJ, Allen JE, Biswas SK, *et al.* Macrophage activation and polarization: Nomenclature and experimental guidelines. *Immunity* 2014;41:14–20.
- 23 Yang R, Mele F, Worley L, *et al.* Human T-bet governs innate and innate-like adaptive IFN- γ immunity against mycobacteria. *Cell* 2020;183:1826–47.

- 24 Hagemann T, Lawrence T, McNeish I, *et al.* "Re-educating" tumor-associated macrophages by targeting NF-kappaB. *J Exp Med* 2008;205:1261–8.
- 25 Liew FY, Xu D, Brint EK, *et al.* Negative regulation of toll-like receptor-mediated immune responses. *Nat Rev Immunol* 2005;5:446–58.
- 26 Sly LM, Rauh MJ, Kalesnikoff J, *et al.* LPS-induced upregulation of SHIP is essential for endotoxin tolerance. *Immunity* 2004;21:227–39.
- 27 O'Neill LAJ, Bowie AG. The family of five: TIR-domain-containing adaptors in Toll-like receptor signalling. *Nat Rev Immunol* 2007;7:353–64.
- 28 Li Q, Verma IM. NF-kappaB regulation in the immune system. *Nat Rev Immunol* 2002;2:725–34.
- 29 Bonizzi G, Karin M. The two NF-kappaB activation pathways and their role in innate and adaptive immunity. *Trends Immunol* 2004;25:280–8.
- 30 Carmody RJ, Ruan Q, Palmer S, *et al.* Negative regulation of toll-like receptor signaling by NF-kappaB p50 ubiquitination blockade. *Science* 2007;317:675–8.
- 31 Yarchoan M, Xing D, Luan L, *et al.* Characterization of the immune microenvironment in hepatocellular carcinoma. *Clin Cancer Res* 2017;23:7333–9.
- 32 Meng Z, Yang P, Shen Y, *et al.* Pilot study of huachansu in patients with hepatocellular carcinoma, nonsmall-cell lung cancer, or pancreatic cancer. *Cancer* 2009;115:5309–18.
- 33 Miao Q, Bi L-L, Li X, *et al.* Anticancer effects of bufalin on human hepatocellular carcinoma HepG2 cells: roles of apoptosis and autophagy. *Int J Mol Sci* 2013;14:1370–82.
- 34 Sica A, Mantovani A. Macrophage plasticity and polarization: in vivo veritas. *J Clin Invest* 2012;122:787–95.
- 35 Ma Y, Mattarollo SR, Adjemian S, *et al.* CCL2/CCR2-dependent recruitment of functional antigen-presenting cells into tumors upon chemotherapy. *Cancer Res* 2014;74:436–45.
- 36 Pikarsky E, Porat RM, Stein I, *et al.* NF-kappaB functions as a tumour promoter in inflammation-associated cancer. *Nature* 2004;431:461–6.
- 37 Maeda S, Kamata H, Luo J-L, *et al.* IKKbeta couples hepatocyte death to cytokine-driven compensatory proliferation that promotes chemical hepatocarcinogenesis. *Cell* 2005;121:977–90.
- 38 Wei Y, Zhao Q, Gao Z, *et al.* The local immune landscape determines tumor PD-L1 heterogeneity and sensitivity to therapy. *J Clin Invest* 2019;129:3347–60.
- 39 Mantovani A, Allavena P, Sica A, *et al.* Cancer-related inflammation. *Nature* 2008;454:436–44.
- 40 Lawrence T. Macrophages and NF-κB in cancer. *Curr Top Microbiol Immunol* 2011;349:171–84.
- 41 Pardoll DM. The blockade of immune checkpoints in cancer immunotherapy. *Nat Rev Cancer* 2012;12:252–64.
- 42 Qin S, Xu L, Yi M, *et al.* Novel immune checkpoint targets: moving beyond PD-1 and CTLA-4. *Mol Cancer* 2019;18:155.